X Encontro Brasileiro sobre Adsorção
27 a 30 de Abril de 2014
Guarujá - SP

ADSORPTION OF Cu(II), Cd(II), Zn(II), Pb(II) AND Ni(II) BY MESOPOROUS SILICA MODIFIED WITH 4-AMINO-2-MERCAPTOPYRIMIDINE.

A.O. Jorgetto[1]; M. H. P. Wondracek[1]; A. C. P. Silva[1]; S. P. Pereira[2]; R. I. V. Silva[1]; M. J. Saeki[1]; M. A. U. Martines[2]; G. R. de Castro[1]

1- Departamento de Química e Bioquímica – Universidade Estadual Paulista "Júlio de Mesquita Filho" (Unesp)
Distrito de Rubião Júnior – CEP: 18618-970 – Botucatu – SP – Brasil
Telefone: (14) 3880-0611 – Email: xjorgetto@gmail.com
2- Departamento de Química – UFMS
Av. Senador Filinto Muller, 1555 – CEP: 79074-460 – Campo Grande – MS – Brasil

ABSTRACT: A SBA-15 type silica was synthesized via sol-gel. The material's surface had its surface silanized and organofunctionalized with 4-amino-2-mercapto-pyrimidine, and the modified material was characterized through superficial area measurements and FTIR, which confirmed the occurrence of the functionalization. The material had its maximum adsorption capacities evaluated via batch adsorption experiments under optimized conditions for Cu(II), Cd(II), Zn(II), Pb(II) and Ni(II) and the values obtained were 13.0 µmol g^{-1} for Zn(II), 12.3 µmol g^{-1} for Cu(II), 3.45 µmol g^{-1} for Ni(II), 2.45 µmol g^{-1} for Pb(II) and 0.60 µmol g^{-1} for Cd(II). Linearized Langmuir and Freundlich models were applied to the data, and the differences in the adsorption capacities were discussed in terms of Person's soft/hard acids/bases, and the ionic radii of the species.

KEYWORDS: SBA-15 silica; functionalization; solid-phase extraction.

1. INTRODUCTION

In the recent years, several types of silicas have been developed for the most varied finalities. Among such materials, porous silicas have attracted great attention due to the versatility associated to their adjustable morphology and porosity, but also to their potentiality of functionalization, high chemical stability in a great variety of media and temperatures, very high specific superficial area, and to the simplicity of their syntheses via sol-gel method, which allows such materials to be obtained through mild reactional conditions [WALCARIUS and MERCIER, 2010]. The great breakthrough in the development of silica-based materials arose with the insertion of pore templates in the reactional sol-gel media, which allowed such materials to attain very high superficial areas, with controlled morphology [WALCARIUS and MERCIER, 2010].

Due to silicas' extraordinary physicochemical properties, porous silicas have been successfully being applied in environmental research mainly as adsorbent materials. In view of that, many papers have reported their application for the uptake of inorganic and organic compounds from aqueous samples [WALCARIUS and MERCIER, 2010].

Among the target pollutants, heavy metals such as cadmium, lead, mercury and *etc*., have had their removal through solid-phase extraction intensively studied due to their high toxicity and to the threat they pose to living beings and to the environment [WALCARIUS and MERCIER, 2010].

The main approach to apply silicas in the solid-phase extraction of heavy metals is based on the immobilization of molecules containinig Lewis-bases over silica surface. To do so, a common approach is to accomplish the silanization post-synthesis of the silica surface with a silylant agent, but other routes are also available [WALCARIUS and MERCIER, 2010].

The pendant Lewis-bases over the material's surface will for form coordinated

covalent bonds with metal species, sequestering them from the media [WALCARIUS and MERCIER, 2010].

In this work, a SBA-15 mesoporous silica was synthesized and organofunctionalized with 4-amino-2-mercapto-pyrimidine. The material was characterized to uncover its superficial area and porosity, but also the occurrence of the functionalization steps. Afterwards, the material was applied in adsorption experiments with Cu(II), Cd(II), Zn(II), Pb(II) and Ni(II) solutions so that the material's maximum adsorption capacities could be determined.

2. MATERIALS AND METHODS

2.1. Synthesis of the SBA-15 silica

1.5 g of Pluronic P123 (BASF) was added to a HCl solution (pH 1). The mixture was agitated until the total dissolution of the copolymer. Under vigorous stirring, tetraethylorthosilicate (*TEOS*) was added to the mixture which was kept under agitation. At the end of this step, the reactional mixture was kept at rest for 12 h, and then 2.56 mL of a 0.25 mol L^{-1} NaF solution was added to the vessel. After that, an aging process was carried out by maintaining the mixture at rest at 32 °C during 72 h. Finally, the silica particles could be filtered in order to extract the material from the solution, and the copolymer was removed from the material's pores by washing the silica in a Soxhlet system with ethanol and water. The material was stored in a heated chamber at 80 °C so that the solvent could be removed.

2.2. Silanization of the silica surface

Prior to the silanization step, the silica had its surface activated by removing the water adsorbed over its surface. This process was carried out by putting the material in a vacuum chamber at 100 °C and at -150 mmHg for 24 h.

The silanization reaction was then performed in a reflux system under nitrogen atmosphere. Into the reactional flask, 60 mL of *N*,*N*-dimethylformamide (*DMF*) (Fluka, > 99,8 %) was added, and the temperature was adjusted to 120 °C. Afterwards, 1.20 mL of 3-chloropropyltrimethoxysilane (*CPTS*) (Fluka, > 95,0 %) was added to the solvent under agitation, and finally 2.00 g of the activated silica was also added to the flask. The mixture was kept under stirring for 48 h, and then was filter in a Büchner funnel and washed with DMF, acetone and alcohol. The material was taken to a heated chamber at 55 °C for solvent removal and, after dried, it was softly grinded so that its particles could be released. The material obtained in this step was identified as *MS-CPTS*.

2.3. Functionalization of the SBA-15 silica with 4-amino-2-mercapto-pyrimidine

Also in a reflux system and under nitrogen atmosphere, 50 mL of DMF was added and the temperature was adjusted to 120 °C. Afterwards, 0.80 g of the ligand 4-amino-2-mercaptopyrimidine (*AMP*) (Sigma-Aldrich, > 97%) was added to the system and it was agitated until complete dissolution. Posteriorly, all the MS-CPTS obtained in the previous step was added to the mixture and it was kept under agitation for another 48 h. The material was filtered, washed, dried and grinded in the same way as it is described in previous item. After this step it was obtained the material so-called *MS-AMP*.

2.4. Batch adsorption experiments

In order to study the influence of the contact time, pH and initial metal concentration, batch experiments were performed. Each parameter was studied in an univariable mode and the experiments consisted of agitating 0.0200 g of MS-AMP with 1.80 mL of the solutions of each metal in 2 mL Eppendorf tubes. After the established contact time for each condition, the metal solutions were filtered, and the solid-free solution was stored to have its metal amount determined through flame atomic absorption. The adsorption capacity for each condition was determined via FAAS. Then, it was calculated the difference between the initial and final concentration, which enabled to compute the amount of metal ions adsorbed per gram of adsorbent.

3. RESULTS AND DISCUSSION

3.1. Characterization of the materials

Superficial area measurements of the non-functionalized silica (*MS*) provided a specific surface area of 663.18 m^2 g^{-1}. After the functionalization, the superficial area of the material was reduced to 260.99 m^2 g^{-1}, demonstrating that the material's surface was effectively modified.

The nitrogen adsorption isotherms of the crude silica indicated a type IV adsorption isotherm (Figure 3.1) [BRUNAUER *et al.*, 1940; SINGH *et al.*, 1985], which is characteristic of mesoporous materials, and implies in the occurrence of capillary condensation in the interior of the pores. The hysteresis noted between the adsorption-desorption isotherms (Figure 3.1) is a type H2 hysteresis, which indicates that the pores are interconnected among themselves, and that they have an "ink-bottle" shape of irregular sizes [BRUNAUER *et al.*, 1940; SINGH *et al.*, 1985]. This information is in agreement with the pore size measurement (input figure in Figure 3.1), in which it can be observed an average pore diameter of 51 Å, which is comprehended in a range from 31 to 71 Å.

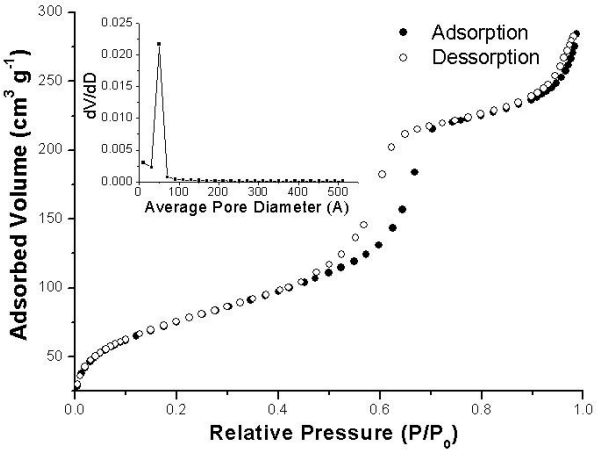

Figura 3.1. Nitrogen adsorption isotherms and average pore diameter for the MS-AMP.

Regarding the FTIR spectra of the materials, we may note from Figure 3.2 (a) the appearance of CH stretching bands in 2955 and 2851 cm^{-1} for MS-CPTS in comparison with the

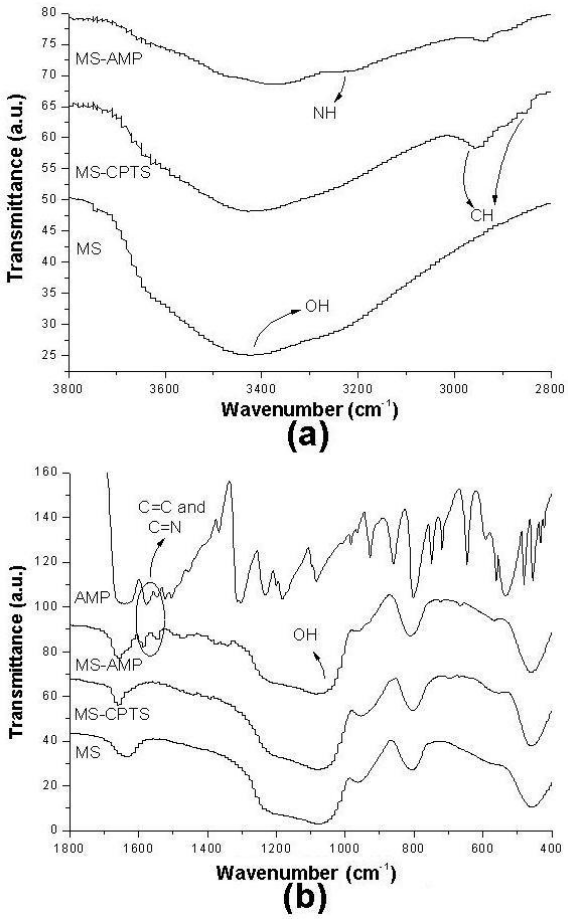

Figura 3.2. Infrared spectra of the non-functionalized mesoporous silica (MS), the silanized mesoporous silica (MS-CPTS), the mesoporous silica modified with the ligand (MS-AMP) and the ligand (AMP). The spectra is divided in two ranges of wavenumber: (a) from 3800 to 2800 cm^{-1}, and (b) from 1800 to 400 cm^{-1}.

MS. These bands were attributed to the carbonic chain of the CPTS, and it confirmed the incorporation of the CPTS structure to the silica's surface. It could also be observed from this same figure that the OH band in 3414 cm^{-1} reduced its intensity after each step of the functionalization, and it may be due to the consumption of the OH groups as the H atoms of such groups are being substituted by the CPTS structure to form Si-O-Si groups. Comparing MS-CPTS and MS-AMP spectra, it can be seen a reduction of the CH bands and also their dislocation to the lower energy direction of the spectrum. This observation is an evidence of the anchoring of the ligand to the material, since the substitution of the Cl atoms of the silylant agent are substituted for the more massive and bulkier structure of the ligand [see

Figure 3.4]. Also, the NH band found in 3200 cm^{-1} [Figure 3.2 (a)] and the absence of the SH bands in the functionalized material's spectrum imply that probably the reaction occurred via the sulphidril group of the ligand rather than via the amine group. Yet, according with Figure 3.3 (b), it could be noticed the appearance of two bands in the MS-AMP's spectrum in 1590 and 1550 cm^{-1}, which exhibited a certain resemblance with the same region of the ligand's spectrum. These bands were attributed to the vibration of C=N and C=C bonds in the ring of the ligand [Figure 3.4 (b)], after the functionalization of the silica, indicating the anchoring of the ligands to the silanized silica [SILVERSTEIN *et al*., 2005].

3.3. Determination of the maximum adsorption capacity

For this experiment, contact time and pH were adjusted to optimize the adsorption of each metal species.

The data collected from the experiments enabled to plot Figure 3.4, and the experimental maximum adsorption capacities may be found in Table 1 [$N_{máx.}$ *(exp.)*].

According to Pearson's concept [PEARSON, 1963], the species Ni(II), Cu(II), Zn(II) and Pb(II) are considered *intermediary acids*, whereas Cd(II) is classified as a *soft acid*. After organizing them in an increasing order of softness, we obtain the following line: Ni(II) < Cu(II) < Zn(II) < Pb(II) < Cd(II). Then, from the obtained N_f values obtained, and according to Figure 3.4, it can be observed that the material presented greater affinity for the intermediary acids Cu(II) and Zn(II) [Figure 3.4 (a)], followed by the also intermediary acids Pb(II) and Ni(II) [Figure 3.4 (b)]. This behavior may be attributed to the presence of nitrogen atoms in the ligand's structure, which have an intermediary-base character, and, therefore, will form more stable coordinated bonds with such type of acids. Also, this fact may also be related to the 3 N : 1 ligand ratio [verify by the molecular structure of the ligand in the Figure 3.4 (b)], in contrast with the ratio 1 S : 1 ligand (in which S possesses a soft-base character), what gives a numerical advantage towards the adsorption of intermediary acids.

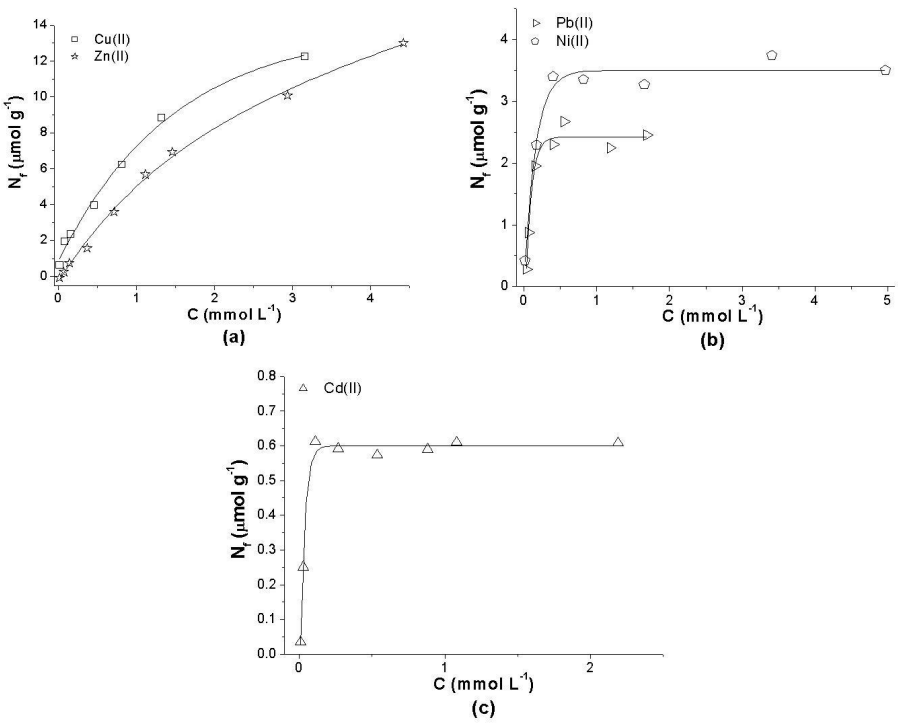

Figura 3.4. Adsorption of Cu(II) and Zn(II) (a), Pb(II) and Ni(II) (b), and for Cd(II) (c) as a function of the initial concentration for the MS-AMP.

Table 1. Parameters of the linearized Langmuir and Freundlich models for the adsorption of Cu(II), Cd(II), Zn(II), Pb(II) and Ni(II), their maximum adsorption capacities and the linear correlation coefficient obtained for each species.

Metal ion	$N_{máx.}$ (exp.)* (µmol g^{-1})	Adsorption model					
		Langmuir			Freundlich		
		K_l (L mmol^{-1})	$N_{max.}$ (cal.)** (µmol g^{-1})	r^2	K_f (L g^{-1})	n	r^2
Zn(II)	13.0	0.133	38.00	0.4677	189.2	1.05	0.9735
Cu(II)	12.3	1.580	14.13	0.9214	18.40	1.96	0.9898
Ni(II)	3.45	16.31	3.610	0.9974	0.049	3.13	0.8129
Pb(II)	2.42	9.785	2.600	0.9782	19.60	2.21	0.6982
Cd(II)	0.60	17.26	0.630	0.9943	95.37	2.33	0.6394

* Maximum adsorption capacities obtained experimentally;
** Maximum adsorption capacities calculated through the Langmuir model.

By its turn, Cd(II) presented the lowest maximum adsorption capacity of all species, demonstrating a low affinity of the material for soft acids. This behavior may be even related to the lower S : ligand ratio (1 : 1), as mentioned previously, and to the greater sterical hindrance soft acids are subjected to in order to coordinate with the S atoms (which present a soft character). As we could see in Section 3.1, the ligand was attached to the material through the S atoms, which caused sterical hindrances for soft acids to be bonded to this site. Yet, this effect is even magnified by the large ionic radius of Cd(II) (0.132 nm).

Sterical hindrances may also be involved with the lower adsorption capacity of Pb(II), in comparison with Cu(II) and Zn(II), since Pb(II) is the softest of the intermediary acids studied [second only to the Cd(II) in order of softness], and, yet, presents the second greater ionic radius [0.103 nm, *vs.* 0.132 nm for Cd(II) ions].

Moreover, in view of the small ionic radius of Ni(II) [0.078 nm (the smallest among the all species)], it would be expected that this species presented the lowest sterical hindrances of all, which could imply in a greater adsorption capacity for Ni(II). Nevertheless, it also presented a maximum adsorption capacity smaller than Cu(II) and Zn(II). This fact may lie on the hard-acid character of Ni(II), since this is the hardest of all intermediary species, probably having greater affinity for harder bases such as alcohols and carboxylic acids. Based on such premise, one may point out that the presence of remnant Si-OH groups on the surface of the MS-AMP [as observed in the spectra of Figure Z (a)] should contribute significantly to the adsorption of Ni(II), but it is important to note that silanol groups are probably found covered by a ligand layer, what impedes the access of Ni(II) ions to such groups.

Aiming to unfold the adsorption model that best fits the material's adsorptive behavior, the obtained data was inserted to the linearized Langmuir and Freundlich models. Their respective parameters may also be found in Table 2.

Taking into account the linear correlation coefficient for each metal species, we may notice that for Cu(II) and Zn(II) (which presented the greatest maximum adsorption capacities), the model that best describes *MS-AMP*'s metal uptake is Freundlich model, whereas for the other metal

Table 2. Comparison between the maximum adsorption capacities (in µmol g^{-1} *) for different sorbent materials.

Material	Zn(II)	Cu(II)	Ni(II)	Pb(II)	Cd(II)	Reference
SM-AMP	13.0	12.3	3.61	2.60	0.63	This study
amino-finctionalized silica nano hollow sphere	_	_	533	467	362	NAJAFI *et al.*, 2012
silica nano hollow sphere	_	_	143	127	185	NAJAFI *et al.*, 2012
Amino-functionalized silica gel	_	_	442	262	284	NAJAFI *et al.*, 2012
SBA-15 silica modified with salicylaldehyde	400	920	360	_	_	MURESEANU *et al.*, 2008
Adsorbent C**	368.2	393.9	_	411.9	_	YANG *et al.*, 2008
Canlerpa lentilifera	40.7	87.7	_	29.0	41.7	PASAVANT *et al.*, 2006
Lignin	172.1	359.9	_	432.0	22.6	GUO *et al.*, 2008
Activated sludge	240.0	299.9	132.6	689.9	250.0	HAMMAINI *et al.*, 2007
Lignocellulosic substrate (wheat bran extract)	245.0	198.0	_	_	_	DUPONT *et al.*, 2005

* some values were converted from the original units to µmol g^{-1};
** mesoporous silica synthesized with cetyltrimethylammonium and tetramethylammonium hydroxide as hybrid surfactant templates by co-condensation with 3-aminopropyltriethoxysilane.
Note: Table 2 was built with the maximum adsorption capacities calculated from Langmuir model, as long as this model had presented a good correlation to explain the adsorptive behavior for here-cited materials. Otherwise, the experimental maximum adsorption capacities were selected to build such table.

species, Langmuir model presented the highest linear correlation coefficient. Perhaps, the lower affinity of ligand towards Ni(II), Pb(II) and Cd(II), associated with the greater sterical restrictions that such species are subjected to, led to a more subtle interaction between such cations and the material's surface, which lead to a fainter superficial interaction, and resulted in the formation of a simple monolayer over the particles. On the other hand, the favorable radius sizes and the higher affinity of Cu(II) and Zn(II) towards the N atoms of the ligand (which are also

more accessible and more abundant than the S atoms) enabled a more effective complexation of such species. This resulted in a greater agreement with the Freundlich model, whose isotherm presents an ever-increasing relation between the metal concentration and the adsorption capacity.

Despite the successful functionalization indicated by the characterization of the material, in general, it presented a low adosorption capacity. A reasonable explanation for such low adsorption may lie in the material's pore shapes, which may not be favoring the access of the metal ions to the adsorption sites in the interior of such pores. The low accessibility to the adsorption sites may also be involved in the slow adsorption kinetics of the material, since these effects may prevent the ions to diffuse inside the pores of the material, increasing the time to reach the kinetic equilibrium.

In Table 2 we may find a comparison between the maximum adsorption capacities of MS-AMP and other studied adsorbent materials for the adsorption of metal species from aqueous media. Such materials include natural sorbents and other organofunctionalized-silicas. As it can be seen from such a table, silicas present a great potential to perform metal uptake from aqueous media. Nevertheless, the electrostatic repulsion compromised drastically the adsorption of MS-AMP towards the metal species, and it presented maximum adsorption capacities much lower than the here-cited sorbents.

4. CONCLUSIONS

The synthesized SBA-15 silica was successfully organofunctionalized with 4-amino-2-mercapto-pyrimidine. Regarding the adsorption experiments, the material presented greater affinity for the intermediary Lewis-acids Zn(II) and Cu(II), followed by Ni(II) and Pb(II). The lowest affinity was found for Cd(II), since it is a soft acid and has the greater ionic radius of all species. Despite the effective functionalization and the material's selectivity for intermediary acids, the maximum adsorption capacities for all the species studied were found beneath the expectations. The material's low efficiency for the solid-phase extraction of metal ions may be due to the low accessibility of the metal ions to the adsorption sites in the interior of the material's pores.

5. REFERENCES

BRUNAUER, S. et al. On a theory of the van der Waals adsorption of gases. *J. Amer. Chem. Soc.*, v. 62, p. 1723-1732, 1940.

DUPONT, L.; et al. Biosorption of Cu(II) and Zn(II) onto a lignocellulosic substrate extracted from wheat bran. *Chem. Lett. 2*. v. 2, p. 165–168, 2005.

GUO, X. Y.; ZHANG, A. Z.; SHAN, X. Q. Adsorption of metal ions on lignin. *J. Hazard. Mater.* v. 151, p. 134–142, 2008.

HAMMAINI, A.; et al. Biosorption of heavy metals by activated sludge and their desorption characteristics. *J. Environ. Manage.* v. 84, p. 419–426, 2007.

MURESEANU, M. et al. Modified SBA-15 mesoporous silica for heavy metal ions remediation. *Chemosphere*, v. 73, p. 1499–1504, 2008.

NAJAFI, M.; YOUSEFI, Y.; RAFATI, A. A. Synthesis, characterization and adsorption studies of several heavy metal ions on amino-functionalized silica nano hollow sphere and silica gel. *Sep. Purif. Technol.*, v. 85, p. 193-205, 2012.

PASAVANT, P. et al. Biosorption of Cu2+, Cd2+, Pb2+, and Zn2+ using dried marine green macroalga *Caulerpa lentillifera*. *Bioresour. Technol.* v. 97, p. 2321–2329, 2006.

PEARSON, R.G. Hard and Soft Acids and Bases. *J. Am. Chem. Soc.*, v. 85, p. 3533 - 3539, 1963.

SILVERSTEIN, R.M.; WEBSTER, F.X.; KIEMLE, D.J. *Spectrometric Identification of Organic Compounds*. 7a Ed., Hoboken: John Wiley e Sons Inc., 2005.

SINGH, K. S. W. et al. Reporting physisorption data for as/solid systems with special reference to the determination of surface area and porosity. *Pure and Appl. Chem.*, v. 57, p. 603-619, 1985.

YANG, H. et al. Hybrid surfactant-templated mesoporous silica formed in ethanol and its application for heavy metal removal. *J. Hazard. Mater.* v. 152, p. 690–698, 2008.

6. ACKNOWLEDGEMENTS

The authors thank FAPESP (2011/14944-5 and 2012/21795-9) and CNPq (302284/2012-5) for the financial support granted.